

## A COINCIDENT-COIL FREQUENCY-DOMAIN ELECTROMAGNETIC PROSPECTING SYSTEM<sup>1</sup>

K. DUCKWORTH<sup>2</sup>, E.S. KREBES<sup>2</sup>, J. JUIGALLI<sup>2</sup>, A. ROGOZINSKI<sup>3</sup> AND H.T. CALVERT<sup>2</sup>

### ABSTRACT

A coincident-coil frequency-domain electromagnetic prospecting device has been developed and its performance investigated by means of scale-model and theoretical studies allied to field tests. The device employs separate transmitter and receiver coils in a configuration which achieves primary decoupling by means of a small offset of the parallel coils axes and a corresponding offset of the coil planes. The radial and axial displacement between the coils is small enough for them to be mounted in the same unit and to behave as though they are coincident. Tests of the device indicate that it offers very strong response to steeply dipping conductors and unusually good spatial resolution of the anomalies due to closely spaced parallel steeply dipping conductors. The device also permits discrimination between high-conductance targets which respond at the inductive limit to separated coil systems. Depth and dip estimates can be obtained in the field from the geometry of response profiles. Profiles obtained over thin isolated conductors located in resistive host rocks using this new device and a conventional horizontal coplanar coil device can be combined to provide separate estimates of the thickness and conductivity of such conductors. Field tests over the Cavendish test range provided responses which were very well-related to the known dimensions of the conductor at that site.

### INTRODUCTION

Exploration systems based on the coincident-coil configuration are familiar in the time-domain or transient electromagnetic (TEM) methods (Velikin and Bulgakov, 1967; Ogilvy, 1983, 1987) but have received little attention in frequency domain. The concept is easily employed in transient systems because of the freedom from primary signal when a step-function primary current is employed. In a frequency-domain, coincident-coil system the extremely strong primary signal would normally preclude the employment of this configuration in the measurement of the very small secondary signals from subsurface conductors other than by the application of unusual technology, such as was described by Morrison et al. (1976). However, if the concept of coincidence is relaxed to allow the transmitter and

receiver coils to occupy separate but closely spaced parallel planes and the coil axes are moved apart, it is possible to achieve complete primary decoupling with the coils at very small separation. This decoupling occurs at the point of polarity reversal between coaxial and coplanar coupling. Depending on the separation of the coil planes, the separation of the coil axes at decoupling can be made as small as required. In air-cored coils, decoupling can be achieved with the coils overlapping each other. Thus the coils of a frequency-domain device can be placed in a configuration in which the coils are at such a small separation that they are effectively coincident while also being inductively decoupled. The consequent freedom from primary signal allows weak secondary signals to be readily detected.

A benefit of a coincident-coil frequency-domain device is that the small, highly portable, dipolar coils which are characteristic of frequency-domain devices allow both the transmitter and receiver coils to be rigidly mounted in one easily portable unit. Thus only a single operator is required.

The very rigid mounting of the two coils which is necessary for this decoupling can only be achieved with small dipolar coils. The device could not be implemented with large nonrigid air-cored coils. A major component of the development effort for this device has been the achievement of the mechanical and thermal stability that this configuration requires.

A second benefit is that with the coils rigidly mounted in the same unit, the device does not suffer from the type of decoupling noise experienced by many moving-source separated-coil systems when operating in mountainous areas.

An additional merit of the coincident configuration can be appreciated in the following arguments. For horizontal coplanar coils of identical dimensions, the geometry of the individual coupling of the coils to the target will be controlled by identical functions (Duckworth et al., 1991). For a vertically dipping perfectly conductive sheet (Wesley, 1958) the coupling function  $k$  for a single coil as it traverses over the sheet has the form shown in Figure 1. The function

<sup>1</sup>Presented at the C.S.E.G. National Convention, Calgary, Alberta, May 5, 1993. Manuscript received by the Editor December 8, 1992; revised manuscript received June 12, 1993.

<sup>2</sup>Department of Geology and Geophysics, The University of Calgary, Calgary, Alberta T2N 1N4

<sup>3</sup>Androtex Ltd., 7225 Harwick Drive, Mississauga, Ontario L4T 3A5

This project was supported by a grant from the Natural Sciences and Engineering Research Council of Canada (NSERC) within the University-Industry Cooperative Research Program (Grant No. CRD-0044894). We are indebted to Dan Forre for his care and diligence in the operation of the scale-modelling system.

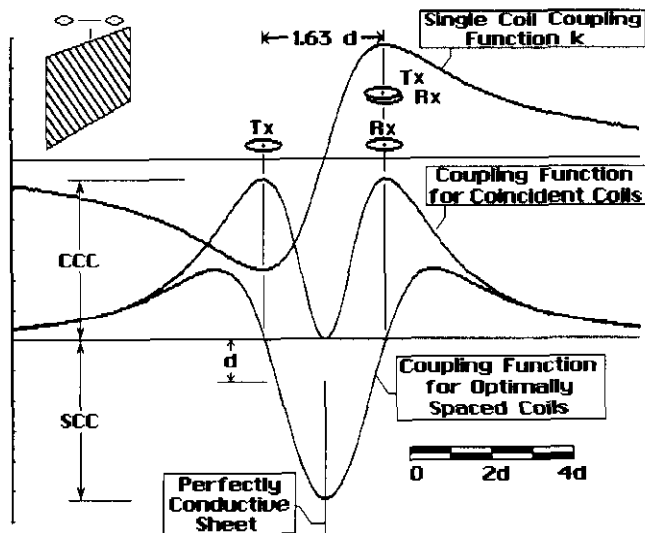


Fig. 1. The coupling function for a single horizontal search coil traversing over a thin vertical perfectly conductive sheet and the resultant coupling profiles for paired coils which are zero spaced and optimally spaced at a separation equal to the separation of the peaks on the single-coil function.

will have this form regardless of whether the coil is a transmitter or a receiver. Thus the coupling between the transmitter and the conductor  $k_{TxC}$  and between the conductor and the receiver  $k_{CRx}$  can be obtained from this single function by sampling at appropriate points on the function which represent the spatially separate locations of the two coils. The combined coupling between the target and two horizontal coils can then be obtained by taking the mathematical product of the individual couplings, i.e.,  $(k_{TxC} \cdot k_{CRx})$ .

Examination of the single coil function  $k$  indicates that optimum combined coupling to the target can be achieved by two possible coil configurations. The first of these will be achieved when the separation of the coils is equal to the separation of the peaks on the single coil coupling function. This separation will allow both coils to come to their individual peak coupling with the target simultaneously. Thus the product of these two components of coupling will also achieve maximum for this separation. Theory (Wesley, 1958) indicates that this optimum separation is  $1.63d$  (or a depth-to-separation ratio of 0.6).

It must be stressed that we are discussing absolute coupling rather than the coupling normalized with respect to primary coupling that is conventionally employed in discussions of frequency-domain devices.

The second configuration for maximum absolute coupling occurs when the coils are coincident, because coincident horizontal coils will inevitably pass through either the positive or the negative peak on the coupling function simultaneously. The magnitude of the product of these two components of coupling will be exactly equal to that provided by the optimally spaced coils. Thus the peak coupling magnitude for the coincident coils denoted CCC in Figure 1 will be equal to the peak coupling magnitude for the separated coils denoted SCC. However, as the separation of the peaks on the

coupling function is controlled by the depth of the target, the separated coils will be optimally separated for only one target depth. In addition, as the lateral separation between the positive and negative maxima on the single-coil coupling function also depends on target type (e.g., this separation is equal to depth  $d$  for a dipole target but  $1.63d$  for a sheet target) the coils will be optimally spaced for only one target type. By comparison, coincident coils must achieve optimum coupling with any type of target at any depth because coincident coils must pass through the peaks on any type of coupling function simultaneously. They may also achieve strong coupling with conductive or magnetic material on the person of the operator. In this respect a coincident-coil device will behave in a manner familiar to the operators of magnetometers in that the operator will have to be clean not only of magnetic material but also of conductive material. It is also clear that responses will be noisy in areas where localized near-surface conductors are common. However, the treatment of such noise should be amenable to spatial filtering as in magnetics, but with the additional feature not available in magnetics that selection of frequency can be used to reduce noise of this type.

Thus the horizontal coincident-coil configuration offers a level of absolute inductive coupling to steeply dipping targets that can only be equalled but never exceeded by separated, horizontal, coplanar coils. The anomaly that coincident horizontal coils will provide over a vertical target will be a symmetrical double-peaked function as shown in Figure 1.

An additional benefit of small coincident coils mounted in a single unit is that they can be operated very easily with their coil planes vertical and with the coil axes directed along the line of traverse. This is a configuration which is not easily implemented with the large transmitter coils used in a TEM system, although it has been implemented in one airborne system (Hogg, 1986). In the search for vertical or steeply dipping tabular conductors this orientation of the coils will provide maximum coupling with the target at the point where both coils pass over the target and become simultaneously coplanar with the target. The anomaly that will be detected by the coils in this configuration will be a single positive peak, examples of which are provided in Figure 4.

The following discussion outlines some of the additional features of the coincident-coil configuration that have become evident as a result of studies that we have conducted. These studies have been based on theoretical and physical modelling allied to the development of prototypes of the device and field tests of those prototypes. A number of aspects of the performance of the device remain to be studied. Our work has covered preliminary tests of models located in free space, in conductive hosts and below conductive overburdens. However, the present discussion will be confined to results obtained over models located in free space. The effects of conductive hosts and overburdens deserve separate and detailed future discussion. We are concerned here only with providing the reader with a view of the immediate and considerable merits of the device, rather than reporting on a fully developed system which will require some time to achieve.

RESPONSE MAGNITUDE

We decided to base evaluation of the coincident-coil system on scale-model and theoretical comparison with the horizontal coplanar configuration because of the large number of studies of the horizontal coplanar coil configuration that have previously been published (e.g., Grant and West, 1965; Lowrie and West, 1965; Ketola and Puranen, 1967; Strangway, 1967; Nair et al., 1968; Hanneson and West, 1984). In our scale modelling, we used the same coils for both configurations. The coincident coils were operated with the coil planes vertical as that will be the logical mode of operation for maximum coupling to steeply dipping targets.

In order to establish that our physical modelling system was operating as expected, we replicated the horizontal coplanar coil work of earlier authors for a vertically dipping thin sheet. These results are presented in Figure 2. Comparison of Figure 2 with the earlier studies of Strangway (1967), Ketola and Puranen (1967) and Nair et al. (1968) shows these results to be in excellent agreement with those studies.

The coincident vertical-coil response over the same target, using the same coils that were used to obtain the coplanar coil results, are shown in Figure 3. The response parameter  $\alpha$  used in Figure 2, with its dependence on coil separation ( $L$ ) can not normally be employed to characterize responses obtained with coincident coils. However, as we were using the same coils and the same target at the same depths, we related the coincident-coil responses to the response parameters used in Figure 2. In addition, we employed what we termed a device-independent response parameter  $\beta$  defined as:

$$\beta = \sigma t^2 \mu \omega,$$

which maintains the dimensionless character of the response parameter by using  $t^2$  instead of  $tL$  so that it does not depend on the coil separation of the device ( $L$ ). These values are presented in brackets in Figure 3. Interpretation of conductor

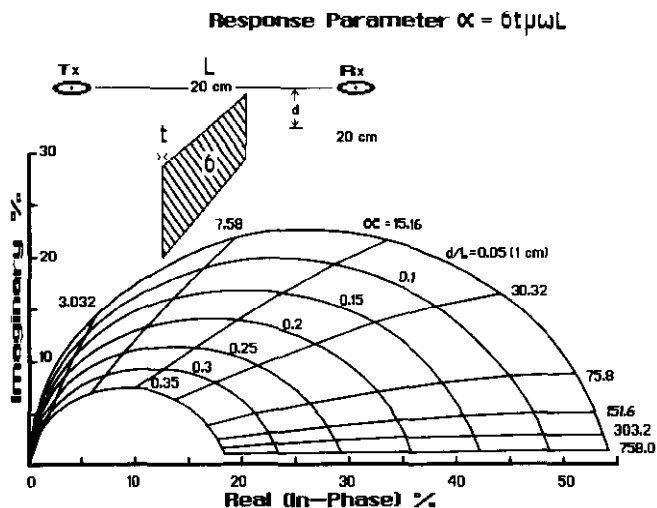


Fig. 2. Anomaly index diagram for horizontal coplanar separated coils over a vertically dipping thin sheet conductor obtained by means of physical scale modelling.

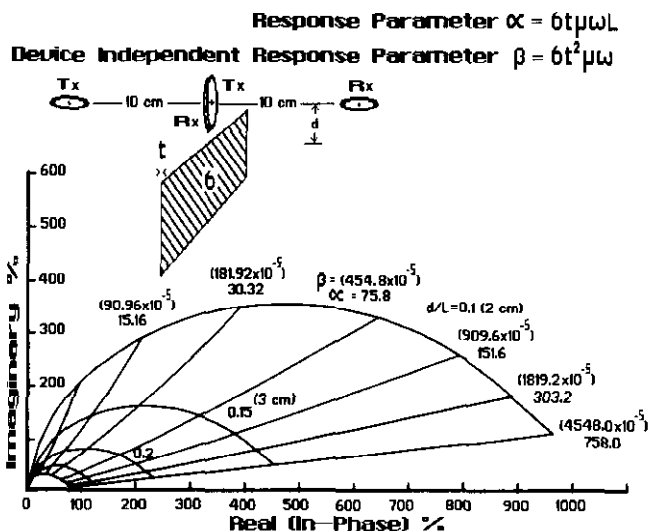


Fig. 3. Anomaly index diagram for vertical coincident coils over a vertically dipping thin sheet conductor. Note that the  $d/L$  values relate to the separated horizontal coplanar coils and that the scale magnitudes were normalized with respect to the primary signal provided by the coils when they were in the horizontal coplanar configuration.

quality based on this parameter yields values of conductance thickness product ( $\sigma t^2$ ) rather than conductivity thickness product ( $\sigma t$ ). As noted by one of the reviewers this suggests that a combination of a coincident-coil survey and a survey using separated coils would permit  $t$  and  $\sigma$  to be determined independently. This is indeed the case and tests with the modelling system show that it works very well for a single conductor located in free space. It does not work for the zone A conductor at Cavendish as discussed later. Users may consider the cost of two surveys to obtain independent estimates of  $t$  and  $\sigma$  are unjustifiable. Theory, however, indicates that the necessary information can be obtained from the coincident-coil system alone if profiles with both vertical and horizontal coil configurations are obtained over the target. This will require the development of response diagrams of the type presented in Figure 3 for the horizontal coincident-coil configuration.

The zero spacing of coincident coils provides no means of expressing depth in a dimensionless form relative to coil separation. Therefore, in Figure 3 we retained the  $d/L$  values as they related to the separation of the coils used in the horizontal coplanar coil study. In TEM interpretation, coil size is commonly used as a reference dimension but the use of small dipolar coils in frequency domain prevents the use of coil size as a reference dimension. A dipolar coil is, from the theoretical point of view, a coil of almost vanishing dimensions. Thus, diagrams of the type shown in Figure 3 can not be used in depth determinations because model depths measured in centimetres can not be converted to full-scale depth if the coil system provides no scalable linear dimension. Diagrams of the type shown in Figure 3 are useful only as a means of evaluating conductor quality in terms of conductance-thickness product but for that use they could be greatly simplified because they do not have to incorporate

depth information. Figure 3 is presented in the format of Figure 2 to facilitate comparisons with the horizontal coplanar-coil system. Depth values can be obtained by alternative means as described later.

It might be argued that practical coils will not respond to each other as dipolar coils at the small separation inherent to this concept but if the coils are inductively decoupled they do not respond to each other at all. The field geometry that will be important is the field experienced by the target conductor, which will be dipolar if the target depth exceeds five coil diameters. This is a condition which will prevail in the majority of exploration environments.

The relative plotting scales in Figures 2 and 3 should be noted. The decoupled coincident coils provided no signal with which the recorded secondary signals could be compared. We therefore normalized all recorded signals with respect to the signal recorded with the same coils horizontal and coplanar in free space at a separation of 20 cm. This provided a direct comparison of secondary signal magnitudes between the two configurations.

The choice of 20-cm separation was dictated by physical constraints of the modelling system. This was the minimum coil separation at which the coils could traverse over the model for depth-to-separation ratios as small as 0.1 without colliding with the model. However, the choice of coil separation did not affect the results displayed in Figures 2 and 3. Had we, for example, employed a separation of 10 cm and halved all depth and thickness values with a corresponding increase in target conductivity by a factor of 4, the coplanar results would, by the requirements of scaling theory (Sinclair, 1948), have been identical to those portrayed in Figure 2. In addition, the coincident-coil responses normalized to the 10-cm separation would have been identical to those shown in Figure 3.

The comparison of Figures 2 and 3 shows that the response of vertical coincident coils was stronger than that of separated horizontal coils for all target depths. For  $d/L = 0.1$  the ratio of the two responses was approximately 20:1. Perfect conductor theory indicates that for truly coincident vertical coils, this ratio should be 52:1 for  $d/L = 0.1$ . This discrepancy between theory and the scale-model data resulted from the relative positioning of the model coils which – to achieve decoupling – were displaced from each other by 2.5 cm radially and 2 cm axially while target depth was 2 cm when  $d/L$  was 0.1. In addition, the coil diameters were 1.5 cm so that they could not behave as coils of vanishingly small dimensions as the theory assumes. The theoretical model was developed to allow the modelling of radial and axial offsets which showed that a combined radial offset of 2.5 cm and an axial offset of 2 cm reduced the ratio to approximately 25:1. A ratio of approximately 25:1 from theory and 20:1 from the scale-model data are in reasonably good agreement, particularly as coil size has not been taken into account in the theoretical model. In the full-scale field environment the configuration of the coils would more closely match the zero radial and axial offset assumed by

theory so that it may be anticipated that a ratio approaching 52:1 for  $d/L = 0.1$  would be more realistic in a full-scale survey.

The much stronger response of the vertical coincident coils is understandable because at peak anomaly the coincident coils were located approximately 2 cm above, and coplanar with, the target. The horizontal coplanar coils at peak anomaly over the same target, at the same depth, were located at a distance of approximately 10 cm from, and perpendicular to, the target, thereby being significantly less well coupled to the target.

For greater target depths the responses of the two coil configurations became closer in magnitude but the coincident response exceeded the coplanar response for all depths as considerations of coupling predict. Thus the coincident-coil configuration is potentially more effective than a separated-coil system for deep exploration.

### SPATIAL RESOLUTION

The relative performance of the coincident vertical coils and the same coils in the horizontal coplanar configuration (20-cm separation) when traversed over a closely spaced group of vertical sheet conductors is shown in Figure 4. The spacing of the conductors was varied from a maximum of 3 cm to a minimum of 1 cm in steps of 1 cm with the depth remaining at 2 cm throughout.

The coincident-coil anomalies provided a clear indication of the presence and relative conductance of three separate conductors when the target spacing was 3 cm. The smaller conductor spacings caused a loss of resolution but even at a spacing equal to half of the depth, the response did indicate that the anomaly was due to a close grouping of conductors. By comparison it would have been very difficult to identify that the coplanar-coil anomalies were caused by a grouping of separate conductors, even at the largest spacing of the conductors. The larger spacing of the coincident-coil profile peaks compared with the actual separations of the conductors was possibly due to mutual interaction between the conductors. However, it may also have been a consequence of the over-scale size of the coils used in the modelling system.

An indication that more than one conductor was involved was provided in the coplanar-coil profiles by the isolated imaginary anomaly caused by the low-conductance target, A, as the leading coil passed over it from the left. This target had little influence on the real component. A corresponding imaginary anomaly would have occurred as the second coil passed over this conductor but that would have occurred when the system also straddled the two high-conductance targets so that this effect was overwhelmed by the response of those targets.

Clearly the vertical coincident-coil configuration achieves spatial resolution of the responses of closely spaced conductors which is significantly better than can be achieved with separated horizontal coils. Figure 4 also shows that the coincident coils indicated the relative conductance of the two strong conductors (B and C) yet the separated horizontal

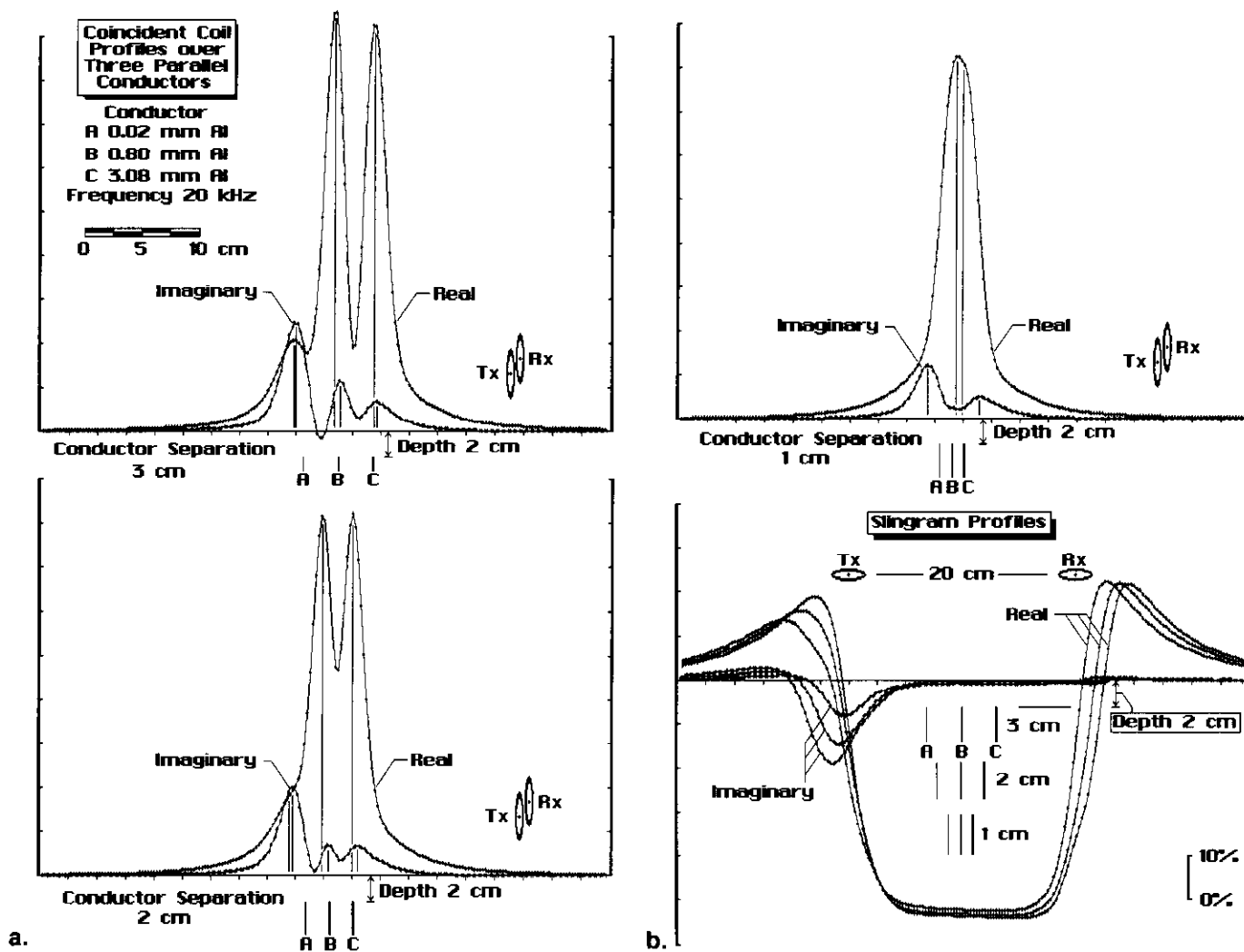


Fig. 4. (a) and (b). The responses of vertical coincident coils when traversed over a closely spaced group of vertically dipping thin conductors demonstrate that the coincident-coil system was able to indicate the presence and relative conductance of all three conductors. The same coils in horizontal coplanar separated configuration could not provide this level of spatial resolution.

coplanar coils responded to the same conductors at close to the inductive limit. This indicates that the coincident coils also provided a level of conductance resolution that the separated coils were unable to match. This is confirmed by the response diagrams of Figures 2 and 3 which show that the coincident-coil response contours for high values of the response parameter in Figure 3 are not crowded against the real axis, thereby allowing high-conductance targets to display distinctly different responses. By comparison, in Figure 2 the crowding of the high-conductance responses against the real axis shows that targets of high conductance produce almost indistinguishable responses when surveyed by separated coplanar coils. It is, however, notable that the low-conductance contours in Figure 3 are more closely bunched than in Figure 2 so that the separated-coil system will be better able to resolve the responses of low-conductance targets than will the coincident-coil system.

A good deal more work remains to be done to fully establish what appear to be remarkable spatial resolving powers of the coincident-coil system.

DEPTH AND DIP DETERMINATIONS

Depth information can be obtained from coincident-coil profiles by an analysis of the geometry of the profiles, much as is done in the interpretation of magnetic profiles. In this context the type of anomaly provided by traversing with the coincident-coil planes horizontal is best suited to this type of analysis. An example of the double-peaked anomaly which horizontal coincident coils provide over a perfectly conductive, steeply dipping sheet is illustrated in Figure 5 for a range of depth values. The depth of the target is very clearly indicated by the separation of the peaks while the dip direction and magnitude are readily determined by the ratio of the peak magnitudes with the enhanced peak lying over the downdip side of the target.

Figure 6 presents a plot of peak separation versus depth to a vertical thin sheet conductor determined by means of physical scale modelling and by perfect conductor theory. The scale-model data inevitably produced separate plots for the real and imaginary components of the response. While the

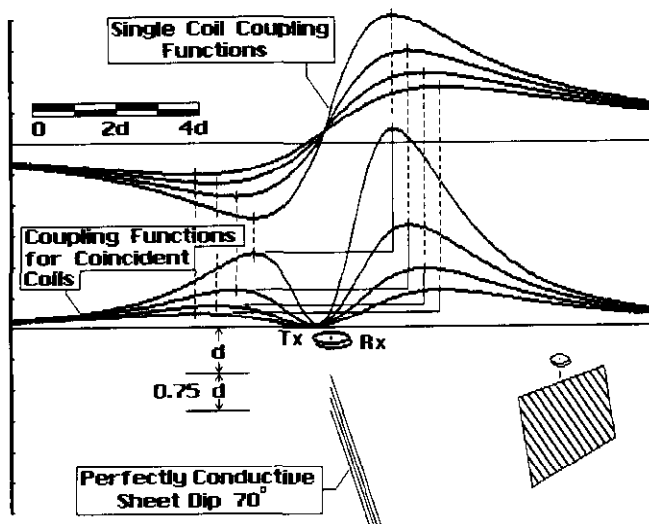


Fig. 5. Depth and dip of conductors can be derived from the geometry of profiles obtained with horizontal coincident coils.

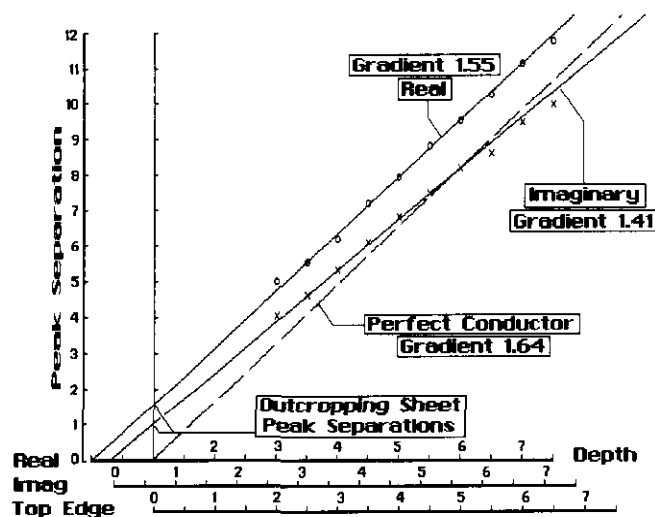


Fig. 6. Depth to the real and imaginary concentrations of the induced current can be determined from profiles obtained with horizontal coincident coils by means of the linear relationships between depth and peak separation displayed here for scale-model and theoretical data.

scale-model data displayed some experimental scatter, we found no evidence that the relationship between depth and peak separation was any other than linear. The perfect conductor theory also indicated a linear relationship and the gradients of the scale-model real component and theoretical data proved to be in good agreement.

The separate real and imaginary intercepts on the zero depth ordinate axis (depth to top edge) arise because the greatest concentrations of real and imaginary components of current lie at different locations below the edge of the sheet. The imaginary current concentration is located closer to the top edge of the sheet than is the real, as discussed by Duckworth (1988) and by Duckworth et al. (1991). Thus, even for an outcropping conductor the peak separation will not be zero. As target conductance was increased so that

both components of current become concentrated closer to the edge of the sheet (not shown), these intercepts diminished but the gradients were unchanged as far as our experiments could determine. Estimation of depth to the individual components of the induced current requires only that the peak separation be divided by the appropriate gradient displayed in Figure 6, regardless of the scale at which the survey is conducted. Thus, for example, with a gradient of 1.55 a real component peak separation of 50 metres would indicate a depth to the real component current of 32.3 metres.

The current locations determined in this way will not provide an indication of the true depth of the top edge of the conductor but they will provide very effective drilling targets. Thus, there is little need to develop a method of obtaining true depth to the top of the conductor although one could be developed. The simple procedure described above has the merit of being applied by the operator in the field. Theoretical modelling indicates that even when the target dip is as low as 60 degrees, the conversion of peak separation to depth using the vertical conductor gradients is still a good depth indicator. A very similar depth determination procedure was described by Duckworth et al. (1991) for application to horizontal coplanar-coil data transformed to remove the effects of coil separation, i.e., to generate synthetic coincident-coil data. In that discussion, it was shown that peak separation as a depth indicator was reliable over wide depth ranges even in circumstances where the conductor dip was quite shallow or where phase was inverted by the presence of conductive overburden.

A coincident-coil survey will normally operate with the coil planes vertical to take advantage of the very good coupling to steeply dipping targets provided by that orientation. However, when a target is detected, the section of traverse over that conductor can be immediately repeated with the coils horizontal so that depth to the induced current components can be estimated by the simple linear procedure described above. In addition, the dip direction and magnitude can be determined by reference to the plot of peak ratio versus dip presented in Figure 7. The results presented in Figure 7 were obtained by physical scale modelling using a target of very high conductance and by perfect conductor theory. It remains to be determined if significant deviations from this relationship will occur as conductance is decreased. The preliminary study we have conducted indicates that use of the plot shown in Figure 7 will provide good dip estimates in a wide range of cases.

#### PRELIMINARY FIELD RESULTS

Results obtained over the zone A conductor at the Cavendish test range (line C) in Ontario, Canada, with our first prototype of the coincident-coil device operating in vertical-coil mode are shown in Figure 8. The results are expressed in amplified coil-output voltage. We intend to adopt normalization to transmitter current in later developments. The imaginary component profiles have been inverted to avoid confusion between the two components.

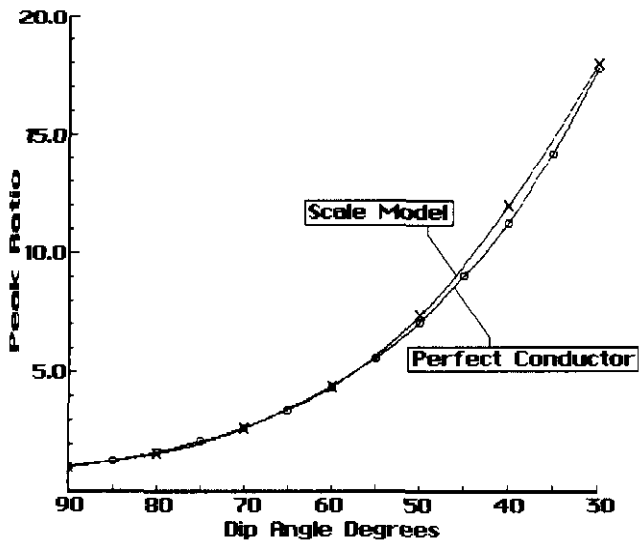


Fig. 7. Dip estimates may be obtained from peak ratio obtained from horizontal coincident-coil profiles as shown in this plot of scale-model and theoretical data for a range of dip values.

These results demonstrate the single peak-type of anomaly to be expected from this mode of operation. Of particular interest is the reduced width of the anomaly at lower frequencies. This suggests that weak conductors which are unresponsive at low frequencies flank the main conductor. The real-to-imaginary ratio moves to higher values for the lower frequencies, which appears to be the converse of what would be expected. However, if weak flanking conductors are present, their influence on the imaginary component would become more significant at higher frequencies. Thus the 300-Hz data appear to provide the best basis for estimates of the quality of the high-grade core conductor. At 300 Hz the data indicates a real-to-imaginary ratio of approximately 2:1. In Figure 3 this real-to-imaginary ratio indicates a device-independent response parameter ( $B$ ) of  $300 \times 10^{-5}$ . For a frequency of 300 Hz this gives a conductance thickness product of 1.27 Sm.

Drilling results for the Cavendish A conductor presented by Williams et al. (1975) show that it is a tabular body 3 m thick consisting of 10% sulphides. It is located at a depth of 1 to 3 m and dips at  $50^\circ$  to the east within a zone of lower grade (2%) sulphides which is approximately 35 m thick. The sulphides are hosted by resistive gneisses. Thus, it appears that the interpretation presented above of a high-grade conductor flanked by lower grade conductors is a good representation of the actual conductor. The conductance thickness product estimate of 1.27 Sm and the drilled 3-m thickness of the conductor indicate a resistivity of  $7 \Omega\text{-m}$  (conductivity 0.14 S/m). This resistivity is comparable to the figure of  $10 \Omega\text{-m}$  employed by Strangway and Koziar (1979) in theoretical models of the zone A conductor. However, electrical logs of drill holes through the high-grade sulphides presented by Mansinha and Mwenifumbo (1983) showed an average resistivity of  $1 \Omega\text{-m}$ . The somewhat high resistivity indicated by our survey suggests that even at 300 Hz the response was not free of the influence of the low-grade halo.

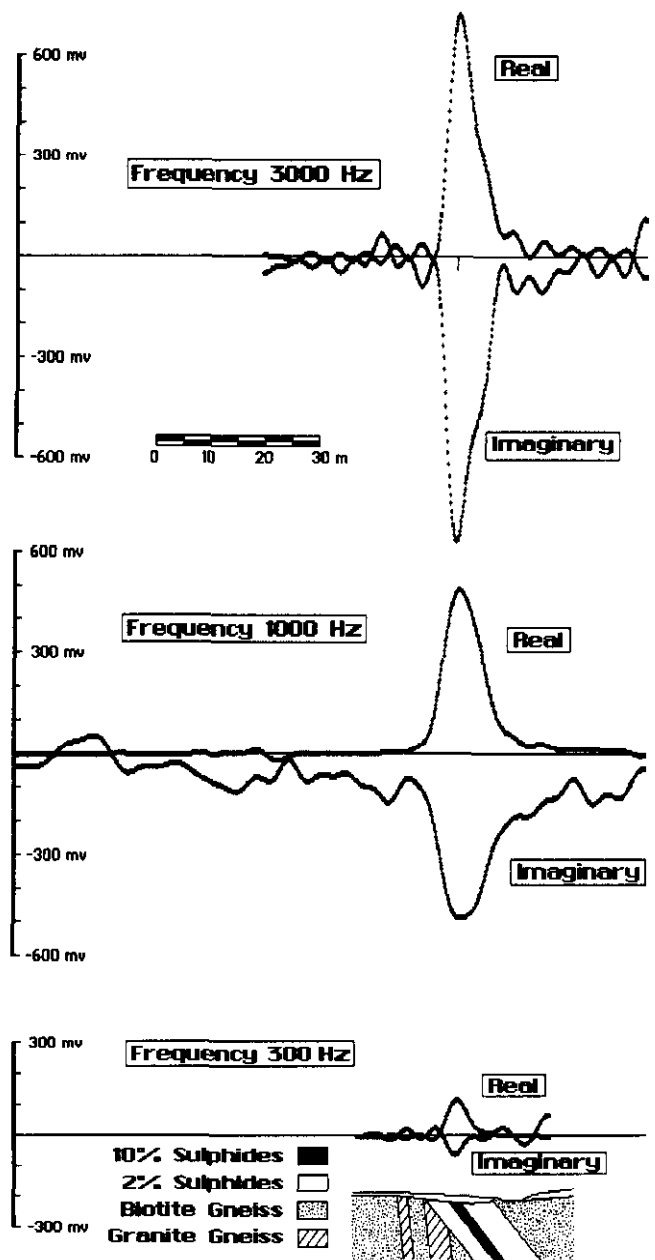


Fig. 8. Vertical coincident-coil profiles obtained over the zone A conductor at the Cavendish test range in Ontario. Note the reduction of anomaly width at 300 Hz which indicates that weak conductors which flank a high-grade core become unresponsive at low frequency. The imaginary component profiles have been inverted to avoid confusion between the two components.

It is also notable that the observed anomalies display an asymmetry, with enhancement to the east. This possibly reflects the dip of the core conductor but it may also represent the fact that the flanking low-grade zone is thicker to the east than the west.

The only horizontal coplanar-coil survey data we have found for this site was obtained at 2400 Hz with a coil separation of 200 ft. These profiles with a real anomaly of 60% and an imaginary of 15% indicate a value of 46 for  $\alpha = \sigma\mu\omega L$  (see Figure 3) which, for this coil separation and

frequency, gives a conductance of 40 S. With the drilled thickness of 3 m this indicates a conductivity of 13.33 S/m. This conductivity is more than an order of magnitude greater than the logged conductivity of the high-grade core (Mansinha and Mwenifumbo, 1983) and approximately two orders of magnitude greater than the 0.14 S/m indicated by the coincident-coil survey. Thus, it appears that the separated horizontal coplanar-coils survey was responding to the much wider low-grade sulphide zone and that this greater width elevated the measured conductance. A horizontal coplanar-coil survey at 300 Hz and at a smaller coil separation would be required in order to have a response compatible with the results of the coincident-coil survey. Consequently, independent estimates of the thickness and conductivity of the target from EM measurements alone were not possible.

### CONCLUSIONS

A good deal of development of the device remains to be done but even at this preliminary stage the following features of the device are clear.

1. Only a single person is required for the operation of this device.
2. Primary coupling is zero and fixed in that condition by rigid mounting of the coils so that the device can not generate decoupling noise in mountainous areas.
3. The coupling of the coincident vertical-coil device to steeply dipping conductors will be stronger than that provided by separated horizontal coils for all conductor depths.
4. The coupling of horizontal coincident coils to steeply dipping conductors will also exceed that provided by horizontal coplanar separated coils unless those coils are set at a separation which is optimum for the target being sought.
5. Spatial resolution of closely spaced steeply dipping conductors is unusually good.
6. Conductance (or, in fact, conductance thickness product) resolution is unusually good for high-grade conductors. However, conventionally separated coils will be better able to discriminate between low-conductance targets.
7. Determination of depth to the induced current is very simple as also is estimation of dip direction and magnitude. These estimates can easily be made by the operator in the field.
8. As the device consists of a single easily portable unit it does not require cut lines to operate.
9. The lack of need for cut lines allied to the smallest possible operating crew appear to offer notably low survey costs.
10. It appears that a means could be developed by which independent estimates of the thickness and conductivity of a target could be derived for single isolated targets in a free-space host.

### REFERENCES

- Duckworth, K., 1988, A modified current filament model for use in the interpretation of frequency-domain electromagnetic data: *Can. J. Expl. Geophys.* **24**, 66-71.
- Calvert, H.T. and Juigalli, J., 1991, A method for obtaining depth estimates from the geometry of Slingram profiles: *Geophysics* **56**, 1543-1552.
- Grant, F.S. and West, G.F., 1965, *Interpretation theory in applied geophysics*: McGraw-Hill Book Co.
- Hannesson, J.E. and West, G.F., 1984, The horizontal loop electromagnetic response of a thin plate in a conductive earth: part II - computational results and examples: *Geophysics* **49**, 421-432.
- Hogg, R.L.S., 1986, The Aerodat multigeometry, broadband transient helicopter electromagnetic system, in Palacky, G.J., Ed., *Airborne resistivity mapping*: Geol. Surv. Can., Paper 86-22, 79-89.
- Ketola, M. and Puranen, M., 1967, Type curves for the interpretation of Slingram (horizontal loop) anomalies over tabular bodies: *Geol. Surv. Finland, Report of Investigations No. 1*.
- Lowrie, W. and West, G.F., 1965, The effect of a conducting overburden on electromagnetic prospecting measurements: *Geophysics* **30**, 624-632.
- Mansinha, L. and Mwenifumbo, C.J., 1983, A mise-a-la-masse study of the Cavendish Geophysical Test Site: *Geophysics* **48**, 1252-1257.
- Morrison, H.F., Dotan, W.M. and Dey, A., 1976, Earth conductivity determinations employing a single superconducting coil: *Geophysics* **41**, 1184-1206.
- Nair, M.R., Biswas, S.K. and Mazumdar, K., 1968, Experimental studies on the electromagnetic response of tilted conducting half-planes to a horizontal-loop prospecting system: *Geoexpl.* **6**, 207-244.
- Ogilvy, R.D., 1983, A model study of the transient electromagnetic coincident loop technique: *Geoexpl.* **21**, 231-264.
- \_\_\_\_\_, 1987, Interpretation of transient EM common-loop anomalies by response characteristics: *Geophys. Prosp.* **25**, 454-473.
- Sinclair, G., 1948, Theory of models in electromagnetic systems: *Proc. Inst. Radio Eng.* **46**, 1364-1370.
- Strangway, D.W., 1967, Electromagnetic parameters of some sulfide ore bodies, in *Mining geophysics: vol. 1, case histories*, Soc. Expl. Geophys.
- \_\_\_\_\_, and Koziar, A., 1979, Audio-frequency magnetotelluric sounding - a case history at the Cavendish geophysical test range: *Geophysics* **44**, 1429-1446.
- Velikin, A.B. and Bulgakov, J.I., 1967, Transient method of electrical prospecting (one-loop version): *Seminar on geophysical methods of prospecting for ore minerals*, U.N.O.
- Wesley, J.P., 1958, Response of dyke to oscillating dipole: *Geophysics* **23**, 128-133.
- Williams, D.A., Scott, W.J. and Dyck, A.V., 1975, Cavendish township geophysical test range: 1973 diamond drilling: *Geol. Surv. Can., Paper 74-62*.